



Article

Expression Profile of New Marker Genes Involved in Differentiation of Canine Adipose-Derived Stem Cells into Osteoblasts

Maurycy Jankowski ¹, Mariusz Kaczmarek ^{2,3}, Grzegorz Wąsiatycz ⁴, Claudia Dompe ⁵, Paul Mozdziak ⁶,
Jędrzej M. Jaśkowski ⁷, Hanna Piotrowska-Kempisty ^{8,9} and Bartosz Kempisty ^{1,4,6,10,*}

- ¹ Department of Anatomy, Poznan University of Medical Sciences, 60-781 Poznan, Poland; mjankowski@ump.edu.pl
- ² Department of Cancer Immunology, Chair of Medical Biotechnology, Poznan University of Medical Sciences, 61-866 Poznan, Poland; markacz@ump.edu.pl
- ³ Gene Therapy Laboratory, Department of Cancer Diagnostics and Immunology, Greater Poland Cancer Centre, 61-866 Poznan, Poland
- ⁴ Department of Veterinary Surgery, Institute of Veterinary Medicine, Nicolaus Copernicus University in Torun, 87-100 Torun, Poland; g.wasiatycz@umk.pl
- ⁵ The School of Medicine, Medical Sciences and Nutrition, University of Aberdeen, Aberdeen AB25 2ZD, UK; claudia.dompe.16@abdn.ac.uk
- ⁶ Prestage Department of Poultry Science, College of Agriculture and Life Sciences, North Carolina State University, Raleigh, NC 27695, USA; pemozdzi@ncsu.edu
- ⁷ Department of Diagnostics and Clinical Sciences, Institute of Veterinary Medicine, Nicolaus Copernicus University in Torun, 87-100 Torun, Poland; jmjaskowski@umk.pl
- ⁸ Department of Toxicology, Poznan University of Medical Sciences, 60-701 Poznan, Poland; hpiotrow@ump.edu.pl
- ⁹ Department of Basic and Preclinical Sciences, Institute of Veterinary Medicine, Nicolaus Copernicus University in Torun, 87-100 Torun, Poland
- ¹⁰ Department of Histology and Embryology, Poznan University of Medical Sciences, 60-781 Poznan, Poland
- * Correspondence: bkempisty@ump.edu.pl; Tel.: +48-61-854-65-67



Citation: Jankowski, M.; Kaczmarek, M.; Wąsiatycz, G.; Dompe, C.; Mozdziak, P.; Jaśkowski, J.M.; Piotrowska-Kempisty, H.; Kempisty, B. Expression Profile of New Marker Genes Involved in Differentiation of Canine Adipose-Derived Stem Cells into Osteoblasts. *Int. J. Mol. Sci.* **2021**, *22*, 6663. <https://doi.org/10.3390/ijms22136663>

Academic Editor: Maria Grazia Cifone

Received: 16 April 2021
Accepted: 16 June 2021
Published: 22 June 2021

Publisher's Note: MDPI stays neutral with regard to jurisdictional claims in published maps and institutional affiliations.



Copyright: © 2021 by the authors. Licensee MDPI, Basel, Switzerland. This article is an open access article distributed under the terms and conditions of the Creative Commons Attribution (CC BY) license (<https://creativecommons.org/licenses/by/4.0/>).

Abstract: Next-generation sequencing (RNAseq) analysis of gene expression changes during the long-term in vitro culture and osteogenic differentiation of ASCs remains to be important, as the analysis provides important clues toward employing stem cells as a therapeutic intervention. In this study, the cells were isolated from adipose tissue obtained during routine surgical procedures and subjected to 14-day in vitro culture and differentiation. The mRNA transcript levels were evaluated using the Illumina platform, resulting in the detection of 19,856 gene transcripts. The most differentially expressed genes (fold change > |2|, adjusted *p* value < 0.05), between day 1, day 14 and differentiated cell cultures were extracted and subjected to bioinformatical analysis based on the R programming language. The results of this study provide molecular insight into the processes that occur during long-term in vitro culture and osteogenic differentiation of ASCs, allowing the re-evaluation of the roles of some genes in MSC progression towards a range of lineages. The results improve the knowledge of the molecular mechanisms associated with long-term in vitro culture and differentiation of ASCs, as well as providing a point of reference for potential in vivo and clinical studies regarding these cells' application in regenerative medicine.

Keywords: adipose; stem cells; RNAseq; transcriptome; analysis

1. Introduction

It is well known that the advancement of modern medicine will be highly dependent on the development of knowledge regarding stem cells [1–6]. While some studies focus on embryonic or induced pluripotent stem cells, the limited knowledge of stem cell regulatory mechanisms, as well as the significant risks associated with their administration, effectively

delays any therapeutic approaches based on these cell types [7,8]. Adult progenitor cells, such as those derived from the bone marrow, have been effectively used in treatment of hematopoiesis-associated diseases (e.g., leukemia) since the 1970s [9,10]. Adult stem cells present a range of advantages over their pluripotent counterparts, such as their ready availability in the adult organism, a narrowed range of differentiation lineages, limiting the possibility of malignant development after implantation, and the possibility of collection without major surgical procedures [11–15]. Furthermore, a significant amount of recent research, especially regarding the treatment of bone- and cartilage-related diseases, focuses on adipose-derived stem cells (ASCs) [1,16,17]. Due to the ease of their extraction during the liposuction procedure, the wide array of works describing the methods of their culture and differentiation and their significant osteogenic and chondrogenic potential, these cells have become one of the most commonly investigated stem cell types, with a number of clinicians attempting to introduce effective treatments based on their autologous transplantation [18,19]. However, the exact molecular mechanisms governing the physiological and non-physiological functions of ASCs during their collection, long-term *ex vivo* culture, cryogenic storage or *in vitro* differentiation are still not entirely known [18]. Therefore, to enable the widespread adoption of this cell type in routine medical practice, a significant amount of wide-scale studies of the processes occurring during the procedures associated with current and potential applications of these cells are still needed to fully discover their actual clinical usefulness, as well as the possible risks associated with their grafting. The canine (*Canis familiaris*) source of stem cells is a relatively widely available model for human studies while also allowing for understanding canine stem cells as a potentially effective treatment in veterinary medicine [4,20,21].

Hence, the present study focuses on next-generation sequencing (RNAseq) analysis of genes with the biggest changes in their expression profile during long-term *in vitro* culture and osteogenic differentiation of canine adipose-derived stem cells (cASCs). The cASCs, isolated during routine surgical procedures, were subjected to culture and differentiation conditions that are, or that could be in the future, employed in procedures of *in vitro* expansion and induction of those cells towards specific lineages prior to autologous grafting. Hence, this study aims to analyze the genes with the most altered expression in the course of these processes, in order to identify new markers associated with the influence of the *in vitro* environment and induced osteogenic differentiation on this type of cells. This knowledge should allow better understanding the molecular mechanisms underlying the processes of ASC preparation for clinical application in veterinary and, potentially, human regenerative medicine.

2. Results

2.1. Flow Cytometry Analysis

Flow cytometry analysis allowed evaluating the expression of the selected available canine ASC markers in the cells of interest to initially confirm their ability before further analysis (Figure 1).

Figure 1 presents the number of acquisition events for fluorescence signals of different intensities. Each of the analyzed antibodies was paired with the corresponding isotype control to correct the obtained results for background fluorescence unassociated with antibody binding. As it is presented in the figure, the two selected positive ASC markers (CD44 and CD90) present a large amount of detection events of larger fluorescence compared to the isotype controls. In turn, negative marker (CD45 and CD34) detection results show that the isotype control and antibody-stained samples show similar levels of fluorescence, confirming the absence of expression of these proteins in the analyzed cells. Overall, the results support the ASC identity of the isolated cell samples.

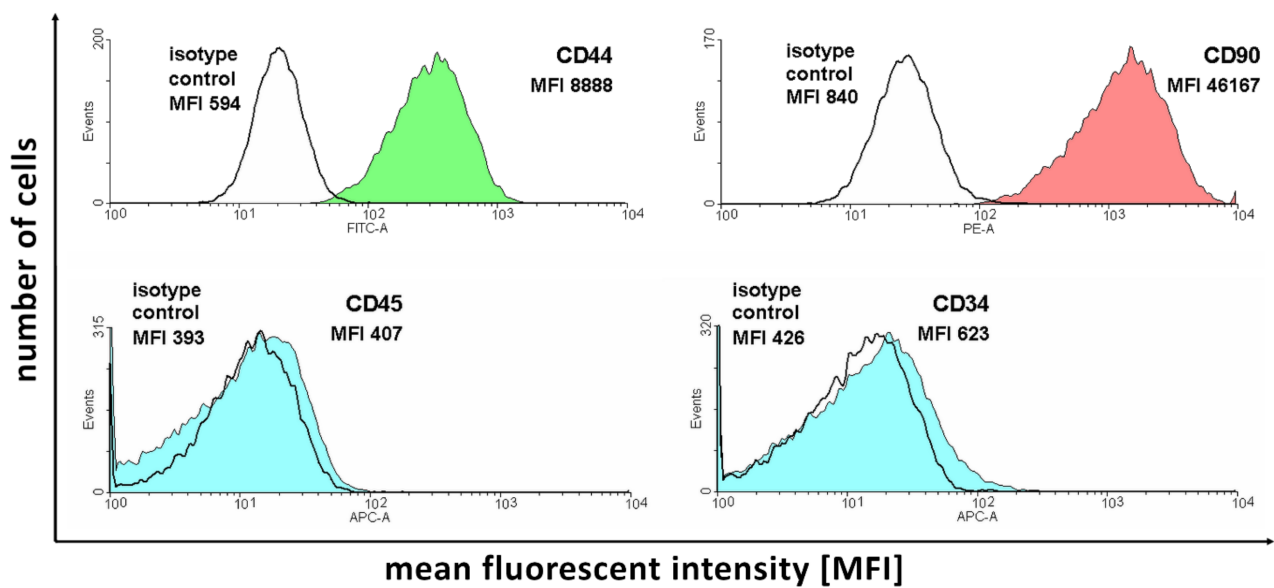


Figure 1. The results of flow cytometry analysis of selected ASC markers in the cell samples subjected to in vitro culture.

2.2. Morphological Evaluation and Osteogenic Differentiation

As it is presented in Figure 2, the initially seeded cells exhibited a fibroblast-like elongated shape, typical for ASC cultures. After several days in culture (day 5), the cells presented a flattened, epithelial-like morphology, resulting from the increase in confluency. On day 13, at the end of the culture period, significant differences between the control and differentiated cells can be observed. While the control sample presents densely packed cells with a morphology typical for late cultures of >90% confluency, differentiated cells are small and more sparsely connected. After Alizarin Red staining, intense red coloring could be observed in the differentiated samples, while controls did not exhibit any color change.

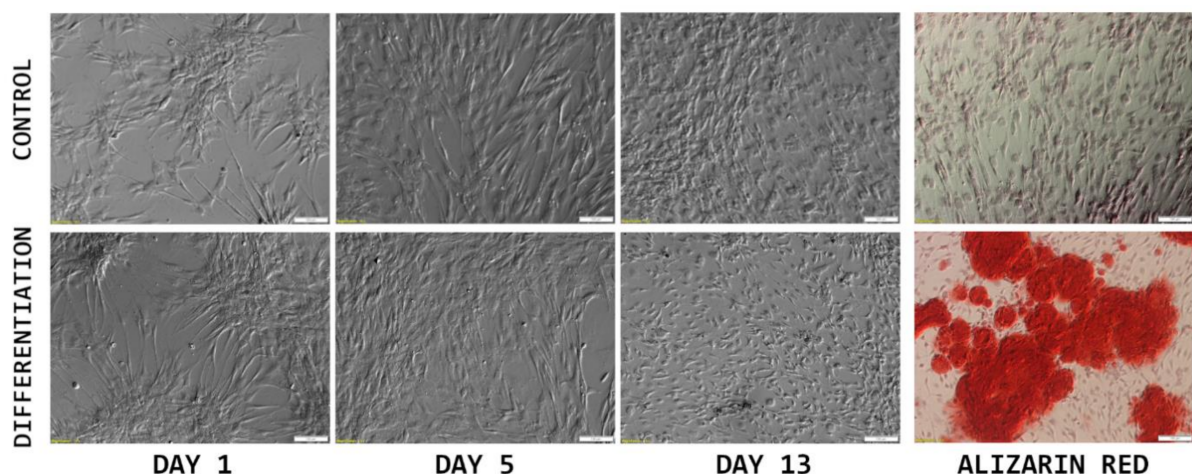


Figure 2. The results of morphological analysis of cASC primary culture (monochrome), combined with Alizarin Red staining photographs (color), to confirm osteogenic differentiation of the cells of interest. Scale bar: 100 μ m.

2.3. RNAseq Analysis

During the initial analysis of the RNAseq results, principal component analysis of the samples was performed to examine variance between the analyzed sample groups and individual samples. The results of the PCA are presented in Figure 3.

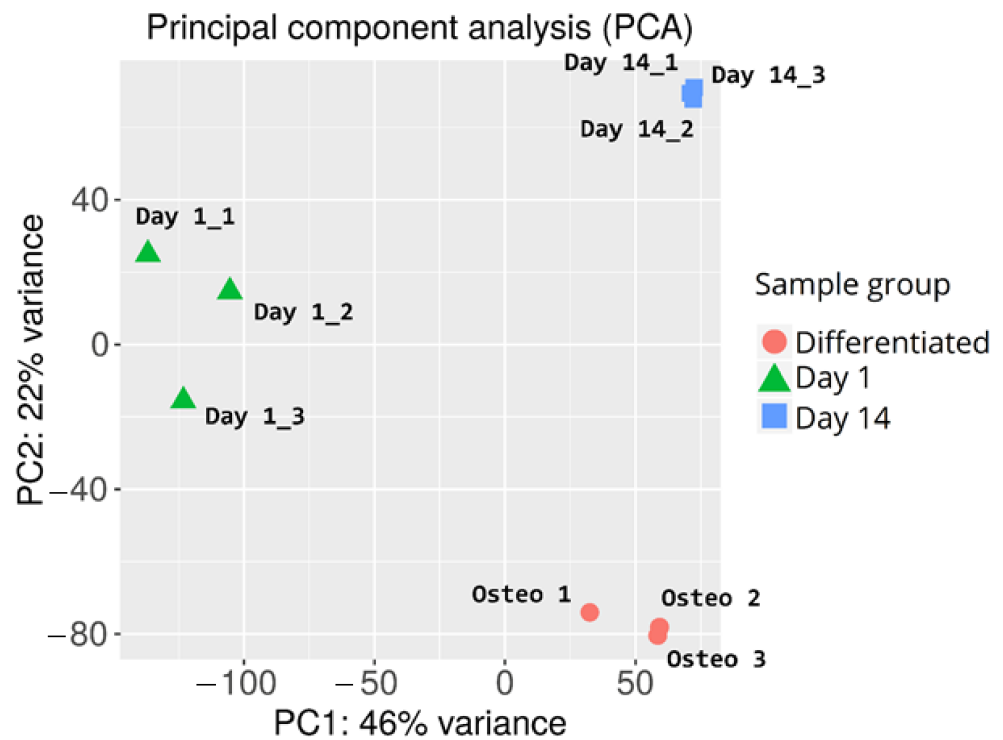


Figure 3. Principal component analysis of cASC samples subjected to RNAseq analysis.

Overall, there is a major variance between the sample groups, with less differences among samples belonging to the same group. This confirms the success of the differentiation procedure, as well as indicating similar gene expression changes evoked by long-term in vitro cultures of individual samples. The in-group variance can be observed in the day 1 control sample group, possibly due to the differences between the canine specimen from which the samples were harvested (e.g., age, condition, administered medication).

Furthermore, genes that were differentially expressed between the analyzed sample groups were selected, based on a fold change of $> |2|$ and an adj. p value of < 0.05 . The initial results of this selection are presented in the form of volcano plots and compiled in Figure 4.

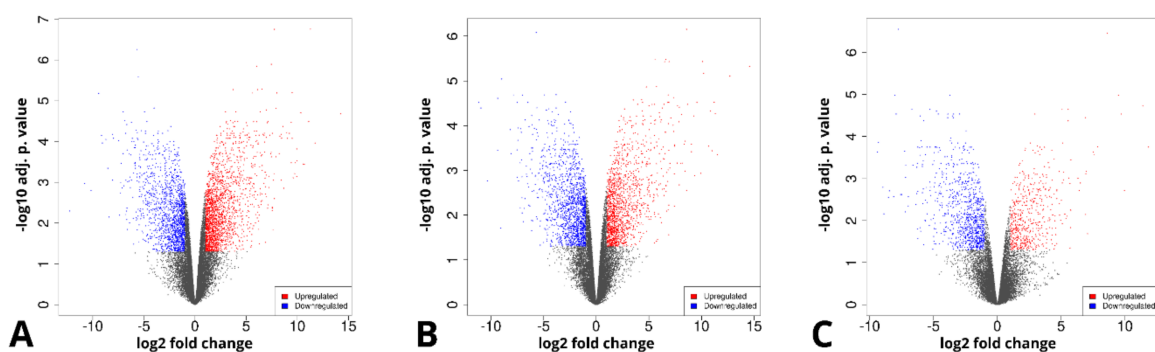


Figure 4. Volcano plots representing the composition of the analyzed sample groups, as well as the proportion and distribution of differentially expressed genes. (A)—day 14 vs. day 1, (B)—differentiated osteoblast vs. day 1, (C)—differentiated osteoblast vs. day 14.

The long-term in vitro culture of ASCs (day 14 vs. day 1) resulted in differential regulation of 3528 genes (1998 upregulated and 1536 downregulated), out of the total of 19,586 genes detected during the analysis (out of which 13,539 were successfully annotated

with an Ensembl gene ID). In turn, similar parameters after osteogenic differentiation were presented by 3087 genes in relation to day 1 (1517 upregulated, 1570 downregulated) and by 1484 genes in relation to day 14 (548 upregulated and 963 downregulated). Out of these three gene sets, the 10 most up- and downregulated genes were selected for further analysis and are presented in the form of log₂FC heatmaps (Figures 5–7) and compiled in Table 1, together with their particular fold changes and adjusted *p* values.

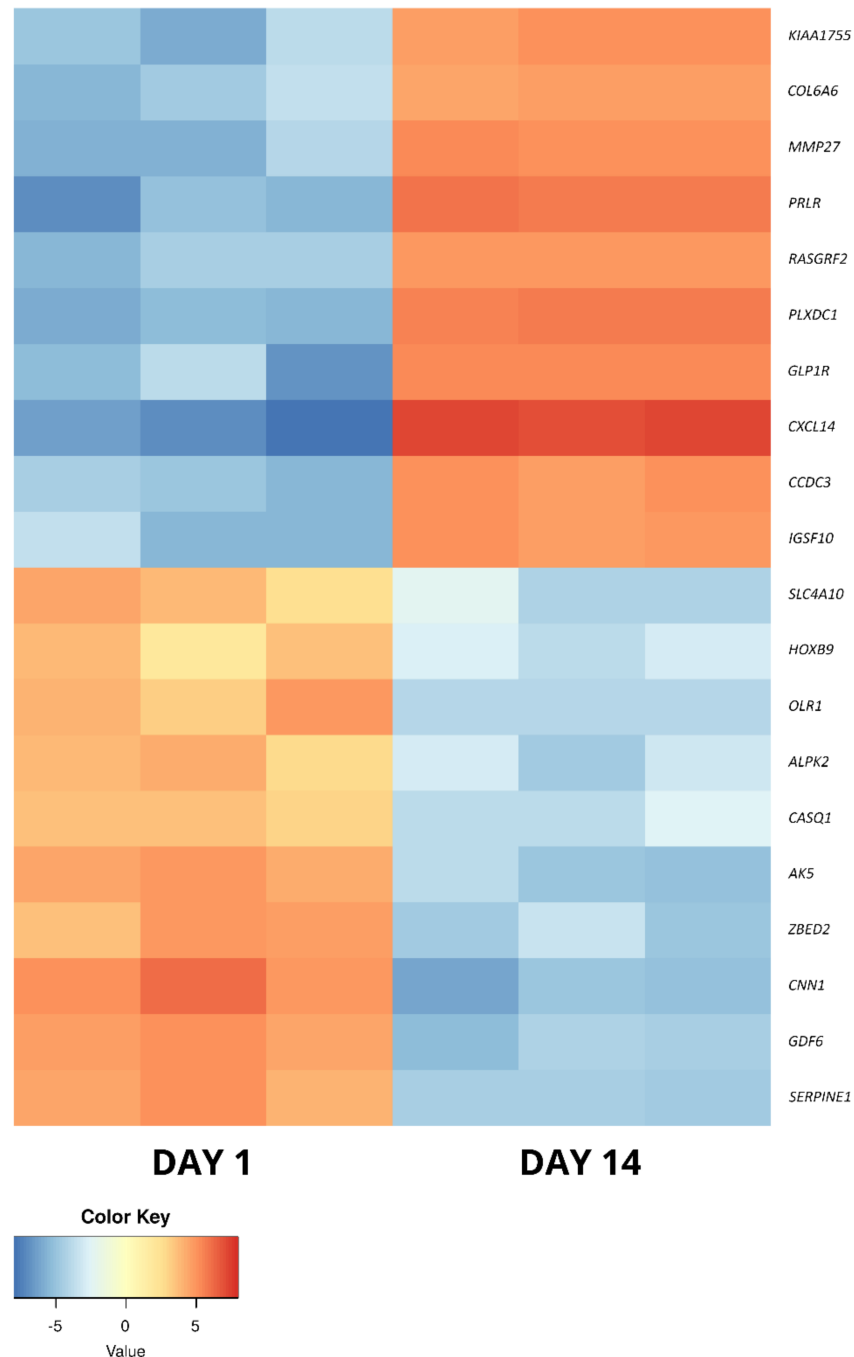


Figure 5. The heatmap representing the changes in the 10 most up- and downregulated genes between day 1 and day 14 of primary cASC culture, presented as log₂FC.

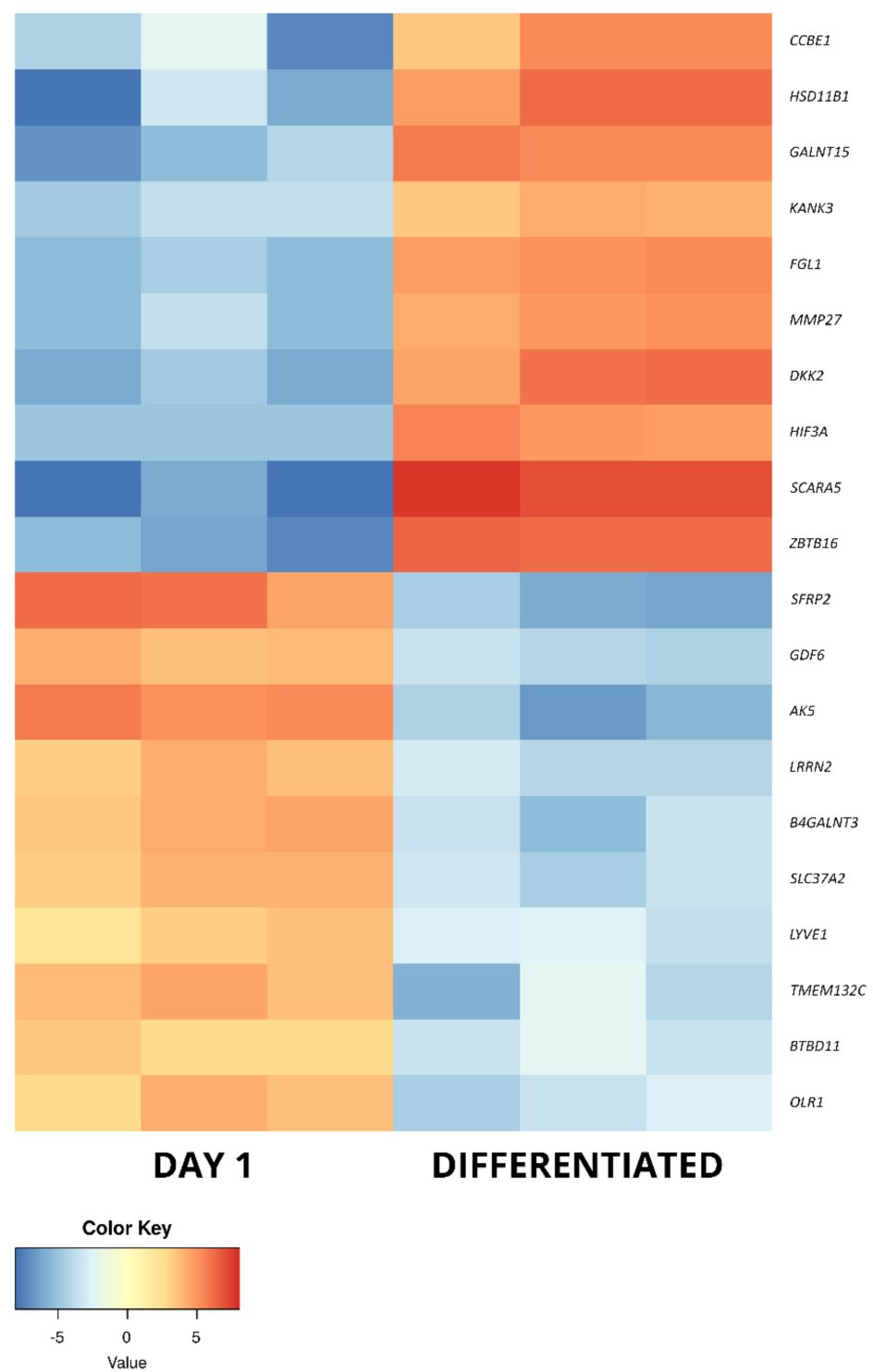


Figure 6. The heatmap representing the changes in the 10 most up- and downregulated genes between day 1 of primary cASC culture and differentiated osteoblasts, presented as log₂FC.

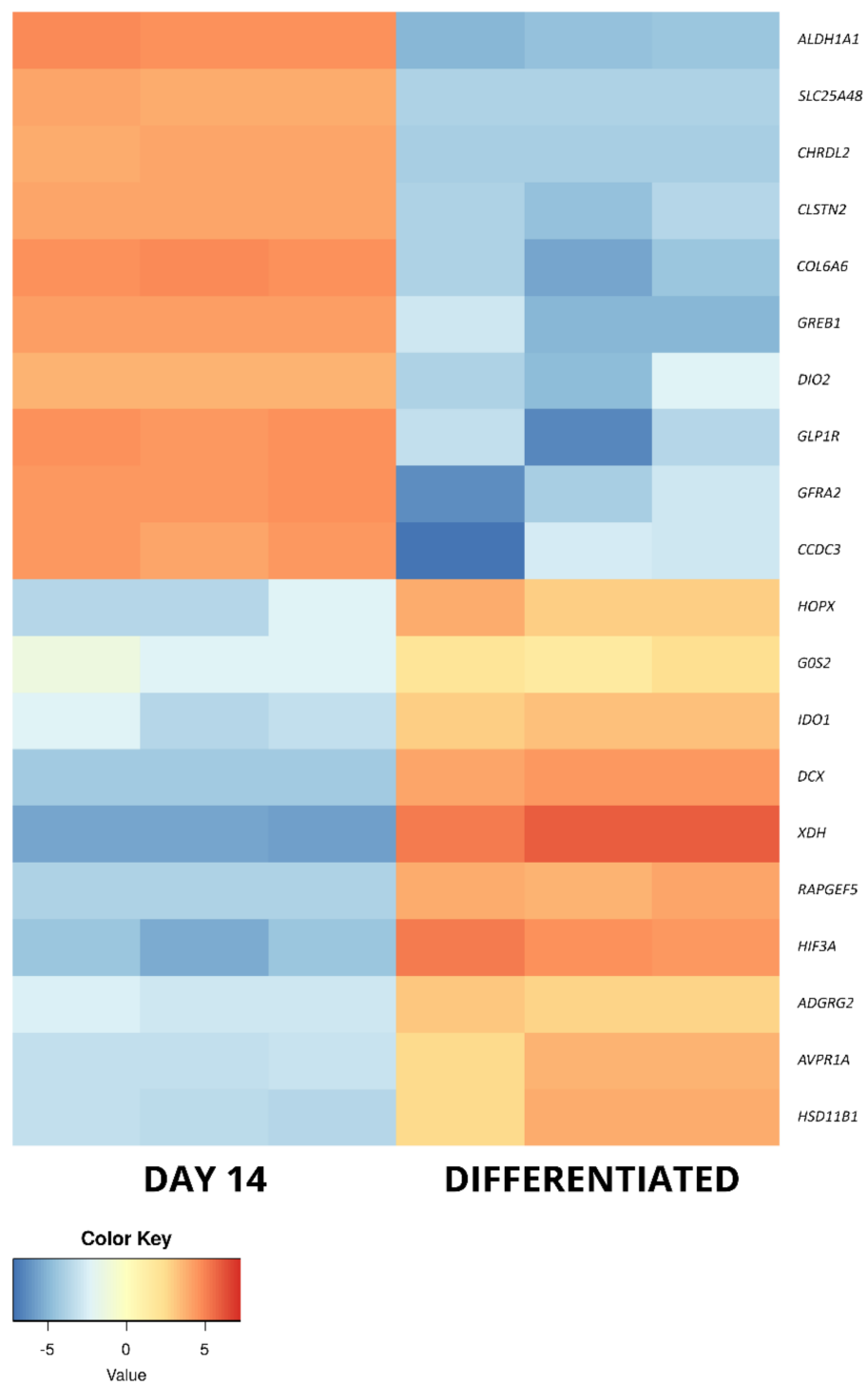


Figure 7. The heatmap representing the changes in the 10 most up- and downregulated genes between day 14 of primary cASC culture and differentiated osteoblasts, presented as log₂FC.

Table 1. The list of differentially expressed genes of interest analyzed in this study. FC—fold change; adj. *p* value—adjusted *p* value.

Day 14 vs. Day 1				
Gene Symbol	FC	Log2FC	adj. <i>p</i> Value	Entrez Gene ID
CXCL14	3.48×10^4	15.1	9.64×10^{-5}	610078
PRLR	4.53×10^3	12.1	3.59×10^{-4}	479363
MMP27	2.70×10^3	11.4	1.31×10^{-3}	489430
PLXDC1	2.53×10^3	11.3	9.06×10^{-6}	491032
RASGRF2	1.98×10^3	11.0	7.71×10^{-6}	610203
GLP1R	1.53×10^3	10.6	9.98×10^{-6}	481778
KIAA1755	1.45×10^3	10.5	5.58×10^{-4}	485868
CCDC3	1.42×10^3	10.5	2.56×10^{-4}	607593
IGSF10	1.03×10^3	10.0	3.54×10^{-3}	477114
COL6A6	8.57×10^2	9.74	7.93×10^{-6}	610649
HOXB9	4.14×10^{-3}	-7.92	3.15×10^{-2}	608958
SLC4A10	3.61×10^{-3}	-8.11	4.24×10^{-2}	478766
ALPK2	3.48×10^{-3}	-8.17	2.47×10^{-2}	483966
CASQ1	3.48×10^{-3}	-8.17	2.00×10^{-3}	608401
OLR1	3.30×10^{-3}	-8.24	3.24×10^{-2}	486694
SERPINE1	1.73×10^{-3}	-9.17	2.19×10^{-2}	403476
AK5	1.63×10^{-3}	-9.26	2.18×10^{-3}	490204
ZBED2	1.60×10^{-3}	-9.29	1.19×10^{-2}	487971
GDF6	5.47×10^{-4}	-10.8	1.10×10^{-3}	100686579
CNN1	4.89×10^{-4}	-11.0	2.89×10^{-2}	484937

Differentiated Osteoblast vs. Day 1				
Gene Symbol	FC	Log2FC	adj. <i>p</i> value	Entrez Gene ID
SCARA5	2.55×10^4	14.6	5.55×10^{-3}	486097
ZBTB16	9.73×10^3	13.2	2.04×10^{-4}	489398
FGL1	4.39×10^3	12.1	4.58×10^{-3}	475617
DKK2	3.64×10^3	11.8	4.36×10^{-2}	478502
GALNT15	1.66×10^3	10.7	1.32×10^{-3}	477056
MMP27	1.65×10^3	10.7	1.18×10^{-2}	489430
HSD11B1	1.45×10^3	10.5	2.40×10^{-2}	449023
HIF3A	1.11×10^3	10.1	6.36×10^{-3}	476429
KANK3	5.85×10^2	9.19	1.09×10^{-2}	476723
CCBE1	4.09×10^2	8.68	4.90×10^{-2}	610092
LYVE1	6.03×10^{-3}	-7.37	2.20×10^{-2}	100855439
TMEM132C	4.44×10^{-3}	-7.82	8.64×10^{-3}	403528
BTBD11	4.34×10^{-3}	-7.85	1.86×10^{-3}	481292
SLC37A2	4.22×10^{-3}	-7.89	4.85×10^{-3}	489303
OLR1	3.64×10^{-3}	-8.10	4.15×10^{-2}	486694
GDF6	3.39×10^{-3}	-8.20	1.86×10^{-3}	100686579
B4GALNT3	2.73×10^{-3}	-8.51	9.29×10^{-3}	486751
LRRN2	1.52×10^{-3}	-9.36	8.64×10^{-3}	488564
SFRP2	4.25×10^{-4}	-11.2	3.41×10^{-2}	475471
AK5	3.90×10^{-4}	-11.3	3.40×10^{-3}	490204

Differentiated osteoblast vs. Day 14				
Gene Symbol	FC	Log2FC	adj. <i>p</i> value	Entrez Gene ID
XDH	4.26×10^3	12.1	3.61×10^{-3}	483028
HIF3A	1.89×10^3	10.9	6.74×10^{-3}	476429
DCX	3.89×10^2	8.60	8.85×10^{-4}	612950
HOPX	2.31×10^2	7.85	4.04×10^{-2}	100855799
RAPGEF5	1.88×10^2	7.56	2.47×10^{-2}	100855786
HSD11B1	1.32×10^2	7.05	3.15×10^{-2}	449023
IDO1	1.08×10^2	6.76	8.60×10^{-3}	475574
AVPR1A	97	6.60	1.59×10^{-2}	481142
ADGRG2	60.6	5.92	5.00×10^{-4}	491763
G0S2	54.7	5.77	2.39×10^{-2}	609704
DIO2	5.34×10^{-3}	-7.55	2.37×10^{-8}	490813
CCDC3	4.72×10^{-3}	-7.73	3.49×10^{-4}	607593
SLC25A48	4.65×10^{-3}	-7.75	5.44×10^{-5}	481518
CHRD2	4.08×10^{-3}	-7.94	1.97×10^{-6}	609312
CLSTN2	3.17×10^{-3}	-8.30	5.39×10^{-6}	477093
GLP1R	2.74×10^{-3}	-8.51	1.15×10^{-5}	481778
GFRA2	2.58×10^{-3}	-8.60	5.41×10^{-5}	609172
GREB1	1.84×10^{-3}	-9.08	9.19×10^{-5}	610007
ALDH1A1	1.38×10^{-3}	-9.50	9.19×10^{-5}	476323
COL6A6	8.90×10^{-4}	-10.1	9.68×10^{-6}	610649

Furthermore, some genes were differentially expressed between multiple analyzed sample groups (Table 2).

Table 2. The list of genes that exhibited differential expression in multiple comparisons between sample groups, with the direction and extent of expression change compared in the form of log2 fold change.

	Log2FC		
	Day 14 vs. Day 1	Osteoblast vs. Day 1	Osteoblast vs. Day 14
<i>AK5</i>	−9.26	−11.30	
<i>CCDC3</i>	1.05		−7.73
<i>COL6A6</i>	9.74		−10.10
<i>GDF6</i>	−10.80	−8.20	
<i>GLP1R</i>	10.60		−8.51
<i>HIF3A</i>		10.10	10.90
<i>HSD11B1</i>		10.50	7.05
<i>MMP27</i>	11.40	10.71	
<i>OLR1</i>	−8.24	−8.10	

Moreover, the differentially expressed gene of interest sets were uploaded to the STRING database to analyze their predicted interactions. The results of this analysis are presented in Figure 8.

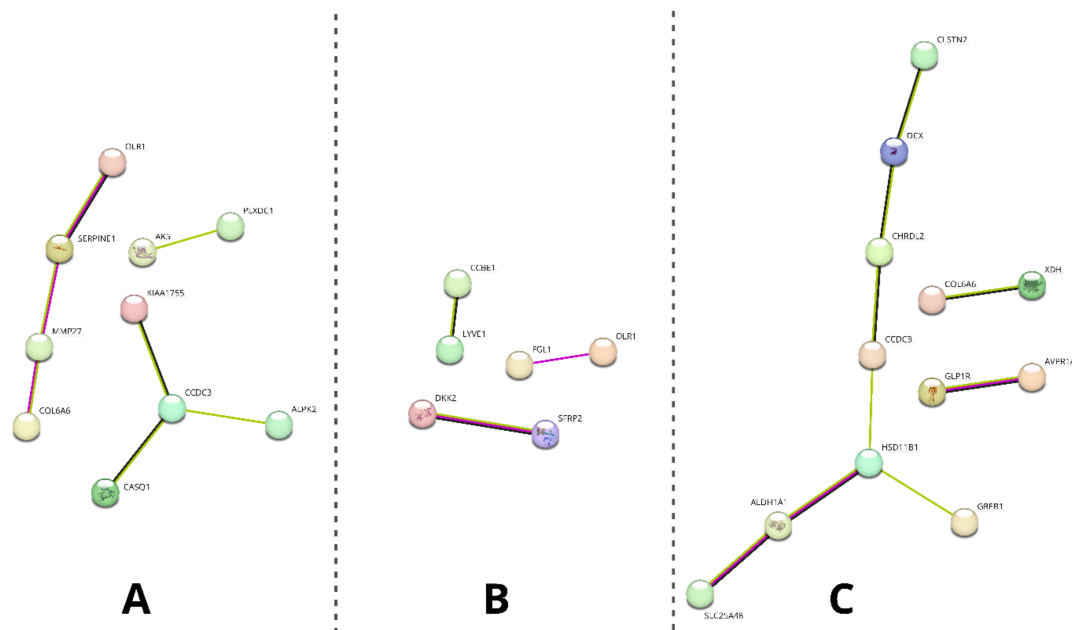


Figure 8. Results of the STRING analysis of predicted interactions between protein products encoded by the differentially analyzed genes of interest. The genes not involved in any interactions were excluded from the figure. (A)—day 14 vs. day 1, (B)—differentiated osteoblast vs. day 1, (C)—differentiated osteoblast vs. day 14. Colors of the edges indicate the source of predicted interaction: magenta—experimentally determined, green—textmining, black—co-expression.

As it is presented, different extents of predicted interactions were indicated among the analyzed sample groups (the highest in group C and the lowest in group B). Furthermore, a varying number of genes in each group were excluded from the analysis due to having no predicted interactions (10/20 on day 14 vs. day 1; 14/20 in differentiated osteoblasts vs. day 1; 8/12 in differentiated osteoblasts vs. day 14).

2.4. RT-qPCR Validation

The sample transcript levels of the differentially expressed genes were validated by RT-qPCR using specific primers. The calculated log2FC results are presented as a bar graph in Figure 9.

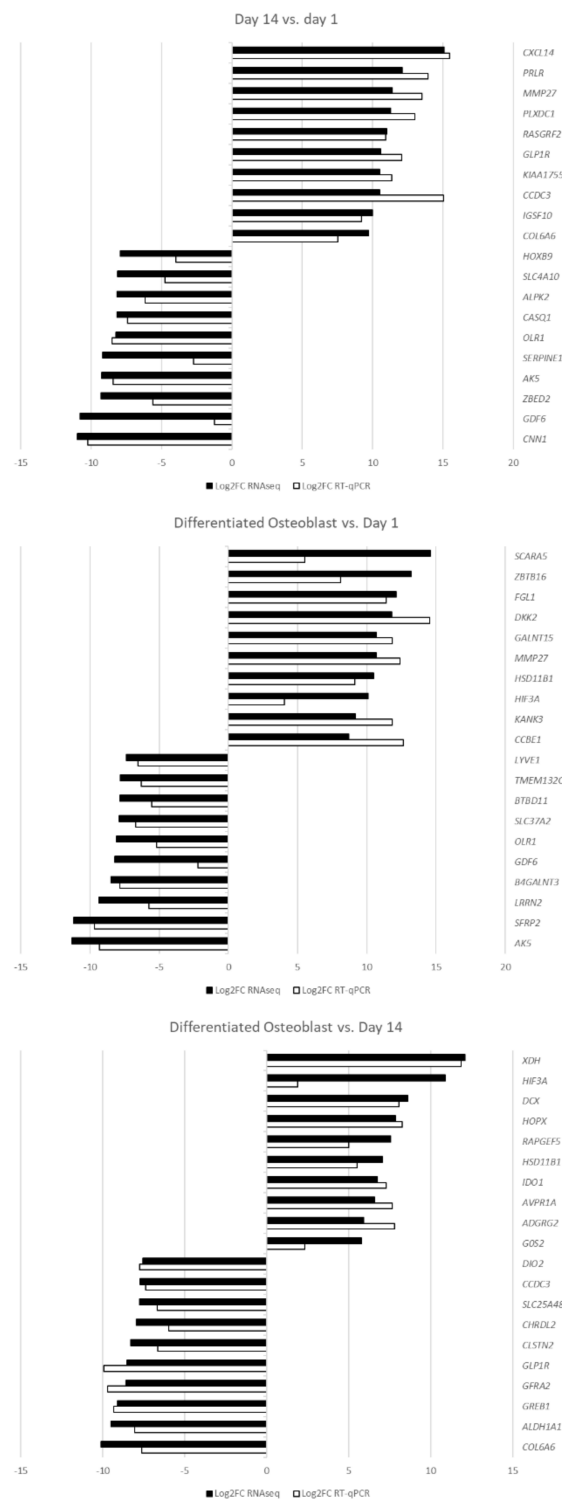


Figure 9. The results of RT-qPCR validation analysis presented as log2FC.

The RT-qPCR analysis confirmed the direction of expression change in all of the samples. For most of the genes of interest, both methods showed comparable results, confirming the accuracy of the RNAseq analysis. However, some of the genes, namely, *GDF6*, *HIF3A*, *SCARA5* and *SERPINE1*, showed major differences in the extent of differential expression, most likely due to the differences in accuracy and sensitivity of the methods used. Nonetheless, all of the analyzed genes were validated as differentially expressed at $FC \geq |2|$ and an adj. *p* value of < 0.05 .

3. Discussion

In the presented study, RNAseq analysis was used to determine the transcriptomic changes associated with long-term in vitro cultures of ASCs, as well as their induced osteogenic differentiation. In the present day, next-generation sequencing (NGS) methods, such as RNAseq, allowed deeply investigating the molecular basis of various cell- and tissue-associated processes, especially when it comes to in vitro cultured cells [22]. This is especially important as adult stem cells, especially MSCs, have a significant potential to be differentiated into cells such as osteoblasts, chondrocytes and neuronal-like cells, which makes them particularly desirable in the context of use in regenerative and reconstructive medicine [11]. Complex transcriptomic analysis of cells with potential application in a clinical setting (e.g., ASCs) permits understanding the mechanisms caused by the ex vivo environment to which they are subjected during preparation for their administration [19]. Furthermore, some studies suggest that stem cells subjected to in vitro conditions have the potential for a significant increase in plasticity and even potential differentiation towards lineages unassociated with the tissue of origin [23]. Moreover, there is an increasingly prevalent discussion regarding the potential differentiation of stem cells prior to application, allowing for ensuring their proper lineage progression and minimizing the risk of malignant progression upon patient administration [19,24]. However, a lot of doubt remains about whether such approach would be beneficial for the clinical results [13]. Hence, the NGS approach can be employed to obtain extensive data on the variation in gene expression observed during the usual procedures conducted during clinical administration of stem cells, and to evaluate the process of the included differentiation for future medicinal use [25]. Furthermore, bioinformatical analysis of the results allows identifying the most differentially expressed genes during such processes that could serve as their reference markers of the effects of in vitro culture and induced differentiation on ASCs, for both future follow-up studies and potential clinical evaluation [26].

Firstly, day 14 samples were compared to those collected at day 1 to show the molecular effects of ASC long-term in vitro culture, suggested as a way to increase their concentration and eliminate contamination with other cell types for clinical application [19]. Among the 10 most upregulated genes between these sample groups, eight were previously associated with stem cell-related processes. When it comes to genes showing elevated expression after 14 days of culture, both *CXCL14* and *PRLR* have been described to take part in the general processes of mesenchymal stem cell (MSC) proliferation and differentiation [27,28]. Similar functions have been attributed to *GLP1R* and *CCDC3*, with their participation in the processes of osteogenic and adipogenic differentiation [29–31]. Furthermore, the latter gene's expression was also observed during ASC immortalization, with a possible implication in cancer progression [32]. *PLXDC1* has also been widely described in the context of malignancy, especially metastasis, and has been previously detected during analysis of mesenchymal stem cells [33]. In turn, *RASGRF2* was also detected in previous MSC analyses, particularly in cells derived from the umbilical cord [34]. Moreover, it has been found to play a role in the regulation of stem cell density and neural differentiation during adult neurogenesis [35]. The next gene, *IGSF10*, has been previously detected to be upregulated during osteoblast differentiation, with an implied role in the ossification process [36]. Finally, *COL6A6* has been implicated in the process of vascular smooth muscle cell differentiation from pluripotent progenitors [37]. The remaining most upregulated genes in this comparison, not previously described in the context of stem cells, were *MMP27* and *KIAA1755*. The former encodes a matrix metalloproteinase particularly involved in stromal breakdown, which was connected to the product of *COL6A6* in the STRING analysis [38]. *KIAA1755* has, only as of now, been implied to have a function in the cardiac rhythm and rate, which does not shed further light on its potential role during long-term in vitro culture of ASCs [39]. However, it is suggested that it has a role in the culture-induced differentiation, as the STRING analysis showed a potential interaction of its protein product with that of the previously described *CCDC3*.

The most downregulated genes are all associated with stem cell differentiation. *HOXB9*, a member of the highly conserved and multifunctional homeobox genes' group, was implied in the normal functioning of stem cells [40]. Its abnormal expression, particularly upregulation, was detected in, e.g., colorectal cancer cells [41]. Similar roles were attributed to *GDF6* and *CNN1*, as they were implied in MSC and adipocyte lineage commitment and contractile MSC differentiation, respectively [42,43]. Furthermore, *AK5*, *ALPK2* and *CASQ1* are all associated with pluripotent stem cells. The first of those genes, *AK5*, was indicated as a marker of cells derived from embryoid bodies [44]. In turn, *ALPK2* and *CASQ1* were detected in pluripotent stem cell-derived lineages. The expression of the former was noted in cardiac cell development, while the latter was implicated in neurogenic differentiation [45–47]. The presence of products of two further genes, *SLC4A10* and *SERPINE1*, was detected in the content of mesenchymal stem cell-derived exosomes [48,49]. In turn, *OLR1* encodes a proinflammatory protein that is often observed at low levels in ASCs, with elevated expression in cells obtained from diabetic and obese animals, predisposing them to an adipogenic fate [50]. Finally, *ZBED2* has been implicated in the process of keratinocyte differentiation, with its depletion resulting in a basal phenotype of increased plasticity [51].

In this comparison, a large number of genes participating in the processes of MSC differentiation were majorly upregulated between day 14 and day 1 of primary culture. This fact, together with the downregulation of several genes responsible for plasticity, suggests the potential of ASCs for lineage commitment after long-term in vitro cultures.

In the current study, the most differentially regulated genes after osteogenic differentiation of ASCs were also investigated. The differentiated osteoblasts were compared to the day 1 control cells, as well as those cultured in vitro for 14 days, in an attempt to correct for the expression changes induced solely by long-term culture. When compared to day 1, 4 out of 10 upregulated genes were associated with an osteoblast phenotype. *ZBTB16*, *DKK2* and *HSD11B1* were previously described to take part in osteogenic differentiation, with the last gene of this set also detected in osteoblasts in vivo [52–56]. In turn, *SCARA5* activity was previously reported to prevent osteoblast differentiation, suggesting a potential inhibiting response of ASCs to the inducing medium [57]. Four further genes were associated with an MSC-related process but were previously implicated only in the differentiation towards other mesenchymal lineages. *FGL1* was found to be upregulated in dental pulp stem cells, as compared to osteoblasts [58]. In turn, *GALNT15* was described as upregulated during adipocyte differentiation, while *HIF3A* and *CCBE1* were, respectively, associated with chondrocyte and cardiac phenotypes [59–61]. Among the last two of the analyzed most upregulated genes between differentiated osteoblasts and day 1 ASC culture, *KANK3* was linked to cancer processes as a tumor suppressor gene, while *MMP27* was already detected to be upregulated after long-term in vitro culture, suggesting its overexpression is not directly connected to the differentiation process [62,63].

Among the most downregulated genes in osteoblasts vs. day 1 of culture, 9 out of 10 were previously described in the context of stem cells. Among them, three (*OLR1*, *GDF6* and *AK5*) presented a similar downregulation after long-term in vitro culture, making it unlikely that they are directly linked to the process of differentiation. Furthermore, four further genes were found to be expressed in MSCs. *BTBD11* was detected in MSCs derived from the umbilical cord, while *SLC37A2* is expressed by bone marrow- and hematopoietic stem cell-derived lineages [34,64]. In turn, *B4GALNT3* was found to be upregulated in 3D cultures of MSCs [65]. While *SFRP2* is certainly connected to the mesenchymal differentiation potential, its exact roles seem to be conflicting, with sources reporting its involvement in adipogenic, neurogenic and osteogenic progression ability [66,67]. *LYVE1* has also been implicated in differentiation processes, marking lymphatic-like phenotype transformation in vitro [68]. Finally, while *NLRR2* was noted to be a differentiation suppressor, the only studies reporting on this gene come from research focused on malignant tumor cells [69]. The last gene in this set, *TMEM132C*, is not yet well described in the literature [70]. However, its downregulation after osteogenic differentiation of ASCs might suggest it as a marker of their stemness and/or differentiation into lineages other than osteogenic.

An upregulation of osteoblast markers was evident, coupled with a downregulation in the expression of genes characteristic for other MSC types. However, as some of the most upregulated genes were previously associated with other mesenchymal lineages, their role in the process of in vitro osteogenic differentiation should be reconsidered. Furthermore, significant upregulation of SCARA5 indicates a previously unseen response of ASCs to induce osteogenic differentiation.

Among the genes that were upregulated between differentiated osteoblasts and day 14 in vitro culture, two (*HSD11B1* and *HIF3A*) were also upregulated in relation to day 1. This further supports the notion that they are important in the processes of osteogenic differentiation and not just related to the influence of long-term in vitro conditions. Furthermore, there are three more genes in this set that have been previously associated with osteoblast differentiation. *HOPX* was described to drive osteogenesis through adipogenesis suppression, while *IDO1* is involved in the kynurenine pathway activated during the osteoblast differentiation process [71,72]. In turn, *RAPGEF5* is a major regulator of nuclear translocation of β -catenin, a mechanism important in canonical Wnt signaling pathways that play a significant role in osteogenic differentiation [73]. Among the next two genes associated with stem cells, *G0S* was found to maintain quiescence of hematopoietic progenitor cells, while *DCX* is a known marker of central nervous system progenitor cells [74,75]. Furthermore, both *XDH* (downregulated in liver tumors) and *AVPR1A* (upregulated in prostate cancer) have been implicated in the activity of cancer-related stem cells [76,77]. The final gene of this set, *ADGRG2*, does not seem to have any association with stem cell-related processes, only being described in recent studies as a marker of male fertility [78]. However, STRING analysis indicated its potential interaction with *GLP1R*, suggesting its possible undescribed participation in the processes associated with long-term in vitro cultures of ASCs.

The final set of the most downregulated genes between osteoblasts and day 14 culture cells contains three genes that were previously detected to be upregulated during the day 14 vs. day 1 comparison (*CCDC3*, *GLP1R*, *COL6A6*). This result suggests that an elevated expression of these genes is only associated with long-term in vitro culture of ASCs and does not play a role during their osteogenic differentiation. Three further genes, *DIO2*, *CLSTN2* and *GREB1*, were previously described to be upregulated in osteoblasts compared to MSCs. However, the obtained results suggest that their change in expression is rather a result of long-term in vitro culture conditions than osteogenic induction of ASCs [79–81]. The next two genes of this set, *CHRD2* and *GFRA2*, are involved in differentiation of chondrocytes and cardiomyocytes, respectively [82,83]. In turn, *ALDH1A1* is a known cancer stem cell marker [84]. The last gene analyzed in this study during this analysis was *SLC25A48*, a member of the *SLC25* mitochondrial transporter protein without a described function in the context of stem cells [85]. However, it is worth noting that it has shown a predicted interaction with *ALDH1A1* in the STRING analysis.

In conclusion, upregulation of several osteogenesis-related genes between differentiated osteoblasts and day 14 of primary culture further confirms the success of the differentiation process, as well as providing further proof of the role of these genes as osteogenic differentiation markers. Furthermore, an expected downregulation of genes related to other differentiation lineages was observed, together with a few genes previously reported to be upregulated in comparison to undifferentiated MSCs, suggesting that some of these genes could be upregulated due to the influence of in vitro culture conditions rather than induced osteoblast differentiation. Overall, this study provides further molecular insight into the processes that occur during long-term in vitro culture and osteogenic differentiation of ASCs. The results allow confirming currently known markers of osteogenic differentiation (e.g., *HSD11B1*, *ZBTB16* and *DKK2*), re-evaluating the roles of some genes in MSC progression towards a range of lineages (e.g., *GALNT15*, *HIF3A* and *CCBE1*) and suggesting new markers associated with the influence of in vitro conditions and induced differentiation on these cells (e.g., *CCDC3*, *GLP1R* and *COL6A6*). Finally, some genes of currently unknown function, such as *KIAA1755* and *TMEM132C*, were found to be among the most regulated during the analyzed processes of ASCs in in vitro culture and osteoblast differentiation, providing a

reference for further studies of their potential role in regenerative and reconstructive medicine as well as translational research.

4. Materials and Methods

4.1. Material Collection

The research material, in the form of small (<1 cm³) samples of adipose tissue, was obtained from a young *C. familiaris* specimen subjected to a routine sterilization procedure at an associated veterinary clinic. The material analyzed in this study is usually discarded after the surgery. Hence, it does not require any additional surgical procedures. Therefore, this study was deemed to be exempt from approval of the local bioethical committee. After collection, the samples were placed in Dulbecco's phosphate-buffered saline (DPBS; Sigma-Aldrich, Saint Louis, MO, USA), supplemented with 1% of antibiotic antimycotic solution (A5955, Sigma-Aldrich, Saint Louis, MO, USA). The material was then stored at 4 °C and transported to the laboratory no longer than 24 h after collection.

4.2. Cell Sample Preparation

The adipose tissue samples were first double washed with ice-cold PBS to remove any remnant blood. Furthermore, they were minced in a Petri dish using sterile surgical blades until homogenous. After such preparation, the samples were subjected to enzymatic digestion in a 1 mg/mL solution of Type I collagenase (Gibco, Thermo-Fischer Scientific, Waltham, MA, USA) for 40 min at 37 °C, with vortexing every 10 min of incubation. Afterwards, the enzyme activity was stopped with addition of 1 mL of fetal bovine serum (FBS, Sigma-Aldrich, Saint Louis, MO, USA), and the sample was centrifuged at 1200× *g* for 10 min. Supernatant liquid was collected from above the resulting cell pellet, which was resuspended in DPBS and centrifuged again at 500× *g* for 10 min. After discarding the supernatant, the obtained cells were resuspended in 4 mL of Dulbecco's Modified Eagle's Medium—high glucose (DMEM, Sigma-Aldrich, Saint Louis, MO, USA), supplemented with 10% FBS (Sigma-Aldrich, Saint Louis, MO, USA), 4 mM of L-glutamine (Sigma-Aldrich, Saint Louis, MO, USA) and 1× antibiotic-antimycotic solution (A5955, Sigma-Aldrich, Saint Louis, MO, USA). The resulting suspension was transferred into 25 cm³ cell culture flasks (two flasks for each canine specimen, in order to ensure the supply of early controls without additional disturbance of differentiation samples).

4.3. Flow Cytometry Analysis

At the beginning of cell culture, a sample of cell-containing medium was collected for antibody staining and flow cytometry analysis. The cells were stained with the following antibodies: rat anti-dog CD44: FITC (11-5440-41, Thermo-Fischer Scientific, Waltham, MA, USA), rat anti-dog CD90: PE (12-5900-41, Thermo-Fischer Scientific, Waltham, MA, USA), rat anti-dog CD45: APC (MCA1042APC, Bio-Rad, Hercules, CA, USA) and mouse anti-dog CD34: Alexa Fluor[®] 647 (MCA2411A647, Bio-Rad, Hercules, CA, USA), as well as respective isotype controls: rat IgG2ak: FITC (11-5440-41, Thermo-Fischer Scientific, Waltham, MA, USA), rat IgG2bk: PE (12-4031-81, Thermo-Fischer Scientific, Waltham, MA, USA), rat IgG2b: APC (MCA6006APC, Bio-Rad, Hercules, CA, USA) and mouse IgG1: Alexa Fluor[®] 647 (MCA928A647, Bio-Rad, Hercules, CA, USA). All of the antibodies and isotype controls were applied at 1:50 dilution, with staining performed according to manufacturer protocols. Stained samples were subjected to flow cytometry using the BD FACSAria[™] cytometer (Becton Dickinson, Franklin Lanes, NJ, USA).

4.4. In Vitro Cell Culture

The initial in vitro cultures (IVC) were conducted for a period of 3 days, or until ~90% confluency was observed, with the exception of early control samples that were harvested for RNA isolation after 1 day of culture. Afterwards, the cells were detached from culture bottles using 1× Trypsin solution (Sigma-Aldrich, Saint Louis, MO, USA) and passaged onto 6-well culture plates. There, they were maintained in DMEM until the 14th day of

culture, with medium changed every 72 h. Furthermore, photographs of the cultures were taken, using an inverted microscope and proprietary software (Ixplore Standard, Olympus, Tokyo, Japan), every 24 h to assess morphological changes of the analyzed cells.

4.5. Osteogenic Differentiation

Three out of six wells of each 6-well culture plate were subjected to osteogenic differentiation. For that purpose, after the initial adherence period, DMEM was replaced with canine osteogenic differentiation medium (Cn417D, Cell Applications Inc., San Diego, CA, USA), supplemented with 1% of antibiotic-antimycotic solution (A5955, Sigma-Aldrich, Saint Louis, MO, USA). The culture was then maintained for a period of 14 days, with medium changed every 72 h. Photographs of the samples were taken every 24 h to monitor the progression of culture. After this period, sample control and differentiated cultures were fixed in Saccomanno solution (Morphisto GmbH, Offenbach am Main, Germany) and stained with Alizarin Red (A5533, Sigma-Aldrich, Saint Louis, MO, USA), according to the manufacturer protocols, in order to ensure the success of osteogenic differentiation. Each 6-well culture plate consisted of material collected from a separate canine specimen. One well out of each technical triplicate was stained with Alizarin Red. The resulting staining and morphological differences of control and differentiated samples were visually confirmed using an optical microscope and proprietary software (Ixplore Standard, Olympus, Tokyo, Japan) and the differentiation medium manufacturer's visual guidelines, in order to ensure the success of the differentiation process. Furthermore, the two remaining culture wells of both control and differentiated samples were pooled together, representing a single set of biological samples.

4.6. RNA Isolation

RNA samples were isolated at three time periods of ASC culture: 1 day of culture (early control), 14 days of culture in DMEM (long-term IVC) and 14 days of culture in osteogenic differentiation media (differentiated osteoblasts). The cells directed for RNA isolation were detached from cultures using $1 \times$ Trypsin solution and placed in 1 mL of TRIzol (Thermo-Fischer Scientific, Waltham, MA, USA). The samples were then frozen at -80 °C. The isolation of RNA was conducted using the TRIzol Plus Purification KIT (12183555, Thermo-Fischer Scientific, Waltham, MA, USA) according to the manufacturer's protocol. The total amount of the collected RNA was then evaluated based on optical density at 260 nm, with its purity determined using the 260/280 nm absorption ratio (NanoDrop 2000 spectrophotometer, Thermo-Fischer Scientific, Waltham, MA, USA). Only samples with RNA content over 1 mg and a 260/280 absorption ratio higher than 1.8 were subjected to further studies.

4.7. RNAseq Analysis

The RNAseq analysis of the samples was performed at CeGaT GmbH (Tübingen, Germany) using the Illumina platform (Illumina, San Diego, CA, USA). The samples consisted of three biological repeats for each of the analyzed culture periods, with three sets of day 1, day 14 and osteogenic samples obtained from three different animals, in order to correct for inter-specimen differences. Before the analysis, additional quality control of the samples was performed using Qubit RNA (Thermo-Fischer Scientific, Waltham, MA, USA) and Bioanalyzer RNA (Agilent Technologies, Santa Clara, CA, USA). RNA integrity numbers (RINs) of the samples were determined at values between 9.3 and 10, allowing for further processing. The cDNA library used for the subsequent analysis was prepared from 100 ng of RNA per sample using TruSeq Stranded mRNA kit (Illumina, San Diego, CA, USA). The sequencing was performed using NovaSeq 6000 (Illumina, San Diego, CA, USA). Afterwards, demultiplexing of the sequencing reads was performed using bcl2fastq (v. 2.20), with adapters trimmed with Skewer (v. 0.2.2) [86]. The trimmed raw reads were aligned to the CanFam3.1 canine genome using STAR (v. 2.5.2b).

4.8. RT-qPCR Validation

The RNA material remaining after RNAseq analysis was subjected to reverse transcription using Transcriptor First Strand cDNA Synthesis Kit (Roche Life Sciences, Basel, Switzerland) and the Eppendorf Mastercycler[®] nexus (Eppendorf AG, Hamburg, Germany), according to the manufacturer protocols. The RT-qPCR validation was then performed on a Lightcycler 96 (Roche Life Sciences, Basel, Switzerland) using Eva Green (SynGen Biotech, Wrocław, Poland) as a detection dye. The final reaction mix consisted of 1 µL of cDNA, 1 µL of forward+reverse primer mix, 2 µL of Eva Green and 6 µL of PCR-grade water. The specific primers were designed based on Ensembl transcript sequences [87], using the Primer3 software (Table 3) [88]. The design process was based on the exon–exon method to avoid potential remnant genomic DNA amplification. Furthermore, the primers were designed to match all of the known protein-coding transcript variants. The results of the analysis were calculated based on the $2^{-\Delta\Delta CT}$ method, with *ACTB* and *HPRT* used as housekeeping genes [89].

Table 3. The sequences of primers used in this study, with Ensembl IDs of the genes used for their design included.

Gene	Ensembl ID	Forward	Reverse
<i>XDH</i>	ENSCAFG00000005609	AGACTGCTCACGGGTCATTC	ACTGCGTCGCCTTTAAACA
<i>HIF3A</i>	ENSCAFG00000045412	AGTGGTGGCTATCTGTGGAC	AGAGTGTCTGCGAGAGTGTG
<i>DCX</i>	ENSCAFG00000018179	CGGAAGCATGGATGAACCTGG	GTCCTGTCTCTCTGGCCT
<i>HOPX</i>	ENSCAFG00000031330	TCAGCAAGGTCAACAAGCAC	TCACGGATCTGCACTCTGAG
<i>RAPGEF5</i>	ENSCAFG00000002731	ATGATGAAGTGGCGACCGTT	CAATCACTCTCGGCGCTG
<i>HSD11B1</i>	ENSCAFG00000011925	CTTCTCCACTTGTGTGACCC	TCCAGGGCACATCTCTCCTT
<i>IDO1</i>	ENSCAFG00000005750	AAACATGTGGACCCAAGCAC	CAGCAGCGAATTCTTCACCA
<i>AVPR1A</i>	ENSCAFG00000000339	CAGCAGCGTGAAGACCATTT	GGTGATGGCTGGGTTTCTG
<i>ADGRG2</i>	ENSCAFG00000012983	ATGGCCTTGGATCCTATGGG	AACGCTCTGTAGGCTTGAA
<i>G0S2</i>	ENSCAFG00000030095	CTGTGAAGCTGTACGTGC	ATCACACGCCCCAGGAAG
<i>DIO2</i>	ENSCAFG000000032243	TCTCCAATGCCTTCTCTG	CTTCACCCAGTTTACCTGC
<i>CCDC3</i>	ENSCAFG00000030997	ACCTGGGAGAAGCGTAACAA	CCAGGGCATTAATGTGTGGG
<i>SLC25A48</i>	ENSCAFG00000001085	GTTTGGCTTCTTCAAGGCCA	CAGGAGAAGCTCAGACAGGG
<i>CHRD12</i>	ENSCAFG000000005475	CTCCAAGCCAGACAACCTA	GGTGTCTTGTCTGGACTGG
<i>CLSTN2</i>	ENSCAFG00000007635	CATTCAAGATCCACGGCCAG	ACTTCTCCAGGCTGTCTCC
<i>GFRA2</i>	ENSCAFG00000010049	CATCTCCATCTGCAACCGTG	GGCTTCTCCCTTGTCTCTGA
<i>GREB1</i>	ENSCAFG00000003579	GAGCACATGACGAAGCAGAG	TCCTTCACTCCCTGCAAIT
<i>ALDH1A1</i>	ENSCAFG00000001791	AGGAGTGTGAAACGGGCTAA	TTTGAGAAAACGGTGGGCTG
<i>SCARA5</i>	ENSCAFG00000008354	CGATGAGGGGAAGATGGGAG	CCCTGCTCTCTCTCTTTG
<i>ZBTB16</i>	ENSCAFG00000013538	GATGACAATGACACGGAGGC	CATGGCTGAAGGACCGAATG
<i>FGL1</i>	ENSCAFG000000032313	AAAACAGCCGCTATGCACAA	CACCTGTAAAACCCAGCC
<i>DKK2</i>	ENSCAFG00000011087	AGAGATCGAAACCATGGCCA	CCCTCTTGGCTGTGGTGA
<i>GALNT15</i>	ENSCAFG00000005887	TGGGCGACATCTACCGAAAT	CAGGGTAGATGTTGGCCAGA
<i>KANK3</i>	ENSCAFG00000029570	ATGGCCAAGTTTGCCTGAAT	CAGCTCTCCACGTAATGTA
<i>CCBE1</i>	ENSCAFG00000000093	CTGCTGGATCTCAGCAGT	TCCACCGTAACTCAGACTT
<i>LYVE1</i>	ENSCAFG00000007580	AGTGCTTGCACTCTCTTCT	TGGACTCTTGGGCTCTTCTG
<i>TMEM132C</i>	ENSCAFG000000006849	ACATCCTTGAGGACAGAGACC	TCCAGTTGAGGGGAGACTTG
<i>BTBD11</i>	ENSCAFG00000001793	CCCAAGCTCAGAGATCA	AGTGTGTAACCTGGGAGA
<i>SLC37A2</i>	ENSCAFG00000010949	TTTTCACTCGCTCTTTGGC	TACGGATGTGTGGGAGTCC
<i>OLR1</i>	ENSCAFG00000013495	TGCTGTGACACTAGGGATCC	TCAAGCTCTGGGTAAGGGT
<i>GDF6</i>	ENSCAFG00000009445	CCAACACCATCACCAGCTTC	CTGGGGATAATTCGAGGCCA
<i>B4GALNT3</i>	ENSCAFG00000015788	ATGACTATACCCGCTGAGC	GGCCCTTGTCTTCTCTGG
<i>LRRN2</i>	ENSCAFG00000009675	AGCTCAACTACTGGCCAAT	AGAGCTGGTGTGGTTGAGA
<i>SFRP2</i>	ENSCAFG00000008353	AAGTTCCTCTGCTCGTCTT	GGCTTCGATACCTTTGGAG
<i>AK5</i>	ENSCAFG00000020380	GTCAAGGAATTAGGCGGCTG	TGGAGGAAGCCGATCATAAC
<i>CXCL14</i>	ENSCAFG0000001084	CTACAGCGACGTGAAGAAGC	ACCACCTGTATGAACCGCTT
<i>PRLR</i>	ENSCAFG00000018782	TGGCAGCAGACTCAGTTTA	ATGACAGCAGAAAGAACGGC
<i>MMP27</i>	ENSCAFG00000015066	TTCCAAACCCATCCGTACA	CTGGAAAGCAGCATCGACTC
<i>PLXDC1</i>	ENSCAFG00000016530	ATGGCCAATTTCAACCTGG	GGCGTCTGATAGTCTGCTT
<i>RASGRF2</i>	ENSCAFG00000008744	TCCAAGAAGCCTCCATCAG	CTTGGAGGCTGTACTGGTGA
<i>GLP1R</i>	ENSCAFG00000001547	GTGTTCCCTGCTGTTTGT	GACACCAGATGCAGATGAC
<i>KIAA1755</i>	ENSCAFG00000008896	ACCCAGGACTCATCAAGGTG	AGGGGTGGCAATCTTTGAGA
<i>IGSF10</i>	ENSCAFG00000008537	ACGCACTGATTACTTCCCA	TGGCTCTCCCATGTGATTT
<i>COL6A6</i>	ENSCAFG00000006035	CTTCCGGGAGAGATGGGATC	TTTATGCGCTCGAATCTCTG
<i>HOXB9</i>	ENSCAFG00000016867	AAGTTTCTTCCGGCCAGTA	CGAGGTAGGGTGGTAGAC
<i>SLC4A10</i>	ENSCAFG00000010242	ATTGATGGTGGCTGCATGC	AGTAACCTTTTGTCTCCGAA
<i>ALPK2</i>	ENSCAFG00000000107	GGCGAGTGGACATTTAGCTG	GAGGTCAGGGTACATCTCGG
<i>CASQ1</i>	ENSCAFG00000012470	GAGTTCCTGCTGACACCTT	CCTCGAAGGCTTGTAAATG
<i>SERPINE1</i>	ENSCAFG00000013909	CCTCCCACTTCTCGGTCTT	TCCCGAGTTTGGTAGAAT
<i>ZBED2</i>	ENSCAFG000000030690	GAGGAGCTGGAGAAGACTGG	CTCTGAGCACCTCTTCTC
<i>CNN1</i>	ENSCAFG00000017326	AGTATGACCACCGAGAGAG	TCGTTGACCTTCTTACCGA
<i>ACTB</i>	ENSCAFG00000016020	TCGAGACTTTCAACACCCCA	CATGAGCTAGTCGGTCAAGT
<i>HPRT1</i>	ENSCAFG00000018870	CCCAGCGTCTGATTAGTGA	AGAGGGCTACGATGTGATGG

4.9. Bioinformatical and Statistical Analysis

The raw counts obtained from the initial analysis contained the numbers of reads assigned to particular geneIDs. These datasets were subjected to normalization using the DESeq2 package (v. 1.24) in R (v. 4.0.3). Normalized gene lists were then annotated with ENTREZ gene numbers using the org.cf.eg.db annotation package included in Bioconductor (v.3.12.0), in order to provide reference for further analyses. The obtained ENTREZ annotated datasets were uploaded to the IDEP.91 interface for further processing and visualization. IDEP is an integrated web application, providing a simple user interface for advanced bioinformatical analysis of RNAseq data [90].

Principle component analysis (PCA) was used to visualize the relationship between samples. For this purpose, EdgeR transformation was used to stabilize the variance across the mean, allowing all of the genes to equally contribute to the distance between samples [91].

Furthermore, differentially expressed gene (DEG) lists were extracted. For that purpose, fold change (FC) was based on the mean expression values of each gene in the three analyzed sample groups. Furthermore, statistical significance of the results was determined based on the *p* value obtained from a Wald test, corrected for multiple comparisons with the use of Benjamini and Hochberg's false discovery rate. The selection of DEGs was therefore based on $FC \geq 2$ and adjusted *p* value ≤ 0.05 . The results of the selection were presented as a volcano plot, on which each point signifies a gene, with the log₂ of the fold change and adj. *p* value presented on the *y* and *x* axes, respectively. For the purpose of this study, the 10 most upregulated and downregulated genes between the sample groups (day 14 vs. day 1; differentiated vs. day 1; differentiated vs. day 14) were selected. The expression of the genes of interest was visualized in the form of heatmaps, with the intensity of each sample's color indicating the extent of the change in expression between sample groups.

Finally, all of the gene of interest lists were uploaded to the STRING (Search Tool for Retrieval of Interacting Genes/Proteins, STRING Consortium, Lausanne, Switzerland) database to determine the predicted interaction between the analyzed genes. The STRING database contains data on protein/gene interactions that have been obtained through experimentation, computational forecasting methods and analyses of the available public literature [92].

Author Contributions: Conceptualization, M.J. and B.K.; methodology, M.J., G.W. and C.D.; software, M.J. and M.K.; validation, M.J.; formal analysis, M.J.; investigation, M.J. and C.D.; resources, G.W. and M.K.; data curation, M.J. and C.D.; writing—original draft preparation, M.J.; writing—review and editing, P.M., H.P.-K., J.M.J. and B.K.; visualization, M.J. and M.K.; supervision, B.K.; project administration, M.J.; funding acquisition, M.J. All authors have read and agreed to the published version of the manuscript.

Funding: This research was funded by the Polish Ministry of Science and Higher Education, grant number DI2017018647.

Institutional Review Board Statement: Ethical review and approval were waived for this study due to the fact that the material on which this study was based is usually a remnant waste of routine veterinary surgeries. Hence, this study does not involve any additional surgical or other medical procedures conducted on animals.

Data Availability Statement: All of the data discussed in this work, if not already included in the manuscript, are available from the corresponding author on reasonable request.

Conflicts of Interest: The authors declare no conflict of interest.

References

1. Im, G.-I. Current status of regenerative medicine in osteoarthritis. *Bone Joint Res.* **2021**, *10*, 134–136. [[CrossRef](#)] [[PubMed](#)]
2. De la Torre, P.; Flores, A.I. Current Status and Future Prospects of Perinatal Stem Cells. *Genes (Basel)* **2020**, *12*, 6. [[CrossRef](#)] [[PubMed](#)]

3. Moncrieff, L.; Mozdziak, P.; Jeseta, M.; Machatkova, M.; Kranc, W.; Kempisty, B. Ovarian follicular cells—Living in the shadow of stemness cellular competence. *Med. J. Cell Biol.* **2019**, *7*, 134–140. [[CrossRef](#)]
4. Kulus, M.; Kulus, J.; Jankowski, M.; Borowiec, B.; Jeseta, M.; Bukowska, D.; Brüssow, K.P.; Kempisty, B.; Antosik, P. The use of mesenchymal stem cells in veterinary medicine. *Med. J. Cell Biol.* **2018**, *6*, 101–107. [[CrossRef](#)]
5. Stefańska, K.; Sibiak, R.; Hutchings, G.; Dompe, C.; Moncrieff, L.; Janowicz, K.; Jeseta, M.; Kempisty, B.; Machatkova, M.; Mozdziak, P. Evidence for existence of molecular stemness markers in porcine ovarian follicular granulosa cells. *Med. J. Cell Biol.* **2019**. [[CrossRef](#)]
6. Jankowski, M.; Dyszkiewicz-Konwińska, M.; Budna, J.; Knap, S.; Bryja, A.; Borys, S.; Kranc, W.; Magas, M.; Jeseta, M.; Bukowska, D.; et al. The differentiation and transdifferentiation of epithelial cells in vitro—Is it a new strategy in regenerative biomedicine? *Med. J. Cell Biol.* **2018**, *6*, 27–32. [[CrossRef](#)]
7. Medvedev, S.P.; Shevchenko, A.I.; Zakian, S.M. Induced Pluripotent Stem Cells: Problems and Advantages when Applying them in Regenerative Medicine. *Acta Naturae* **2010**, *2*, 18–27. [[CrossRef](#)]
8. Jarrige, M.; Frank, E.; Herardot, E.; Martineau, S.; Darle, A.; Benabides, M.; Domingues, S.; Chose, O.; Habeler, W.; Lorant, J.; et al. The Future of Regenerative Medicine: Cell Therapy Using Pluripotent Stem Cells and Acellular Therapies Based on Extracellular Vesicles. *Cells* **2021**, *10*, 240. [[CrossRef](#)]
9. Man, Y.; Yao, X.; Yang, T.; Wang, Y. Hematopoietic Stem Cell Niche During Homeostasis, Malignancy, and Bone Marrow Transplantation. *Front. Cell Dev. Biol.* **2021**, *9*, 14. [[CrossRef](#)]
10. De la Morena, M.T.; Gatti, R.A. A History of Bone Marrow Transplantation. *Hematol. Oncol. Clin. North Am.* **2011**, *25*, 1–15. [[CrossRef](#)]
11. Young, H.E.; Black, A.C. Adult stem cells. *Anat. Rec.* **2004**, *276A*, 75–102. [[CrossRef](#)]
12. Rojewska, M.; Popis, M.; Jankowski, M.; Bukowska, D.; Antosik, P.; Kempisty, B. Stemness specificity of epithelial cells—Application of cell and tissue technology in regenerative medicine. *Med. J. Cell Biol.* **2018**, *6*, 114–119. [[CrossRef](#)]
13. Stefanska, K.; Bryl, R.; Moncrieff, L.; Pinto, N.; Shibli, J.A.; Dyszkiewicz-Konwińska, M. Mesenchymal stem cells- A historical overview. *Med. J. Cell Biol.* **2020**, *8*, 83–87. [[CrossRef](#)]
14. Stefanska, K.; Bryl, R.; Hutchings, G.; Shibli, J.A.; Dyszkiewicz-Konwińska, M. Human umbilical cord stem cells—The discovery, history and possible application. *Med. J. Cell Biol.* **2020**, *8*, 78–82. [[CrossRef](#)]
15. Müller, M.; Czarnecka, J.; Brzeziński, M.; Prus, J.; Kulak, B.; Hołubowski, A.; Stasiak, M.; Borowiec, B.; Bryl, R.; Moncrieff, L.; et al. Current stem cells technologies used in medicine. *Med. J. Cell Biol.* **2020**, *8*, 124–138. [[CrossRef](#)]
16. Gimble, J.M.; Katz, A.J.; Bunnell, B.A. Adipose-Derived Stem Cells for Regenerative Medicine. *Circ. Res.* **2007**, *100*, 1249–1260. [[CrossRef](#)]
17. Mizuno, H.; Tobita, M.; Uysal, A.C. Concise Review: Adipose-Derived Stem Cells as a Novel Tool for Future Regenerative Medicine. *Stem Cells* **2012**, *30*, 804–810. [[CrossRef](#)]
18. Dompe, C.; Wasiatycz, G.; Mozdziak, P.; Jankowski, M.; Kempisty, B. Current clinical applications of adipose-derived stem cells in humans and animals. *Med. J. Cell Biol.* **2019**, *7*. [[CrossRef](#)]
19. Jankowski, M.; Dompe, C.; Sibiak, R.; Wasiatycz, G.; Mozdziak, P.; Jaśkowski, J.M.; Antosik, P.; Kempisty, B.; Dyszkiewicz-Konwińska, M. In Vitro Cultures of Adipose-Derived Stem Cells: An Overview of Methods, Molecular Analyses, and Clinical Applications. *Cells* **2020**, *9*, 1783. [[CrossRef](#)]
20. Cotman, C.W.; Head, E. The canine (dog) model of human aging and disease: Dietary, environmental and immunotherapy approaches. *J. Alzheimer's Dis.* **2008**, *15*, 685–707. [[CrossRef](#)]
21. Shah, K.; Drury, T.; Roic, I.; Hansen, P.; Malin, M.; Boyd, R.; Sumer, H.; Ferguson, R. Outcome of allogeneic adult stem cell therapy in dogs suffering from osteoarthritis and other joint defects. *Stem Cells Int.* **2018**, *2018*. [[CrossRef](#)] [[PubMed](#)]
22. Levy, S.E.; Myers, R.M. Advancements in Next-Generation Sequencing. *Annu. Rev. Genomics Hum. Genet.* **2016**, *17*, 95–115. [[CrossRef](#)]
23. Kranc, W.; Brazert, M.; Ożegowska, K.; Nawrocki, M.M.J.; Budna, J.; Celichowski, P.; Dyszkiewicz-Konwińska, M.; Jankowski, M.; Jeseta, M.; Pawelczyk, L.; et al. Expression Profile of Genes Regulating Steroid Biosynthesis and Metabolism in Human Ovarian Granulosa Cells—A Primary Culture Approach. *Int. J. Mol. Sci.* **2017**, *18*, 2673. [[CrossRef](#)]
24. Si, Y.L.; Zhao, Y.L.; Hao, H.J.; Fu, X.B.; Han, W.D. MSCs: Biological characteristics, clinical applications and their outstanding concerns. *Ageing Res. Rev.* **2011**, *10*, 93–103. [[CrossRef](#)] [[PubMed](#)]
25. Ku, C.S.; Naidoo, N.; Wu, M.; Soong, R. Studying the epigenome using next generation sequencing. *J. Med. Genet.* **2011**, *48*, 721–730. [[CrossRef](#)] [[PubMed](#)]
26. Dyszkiewicz-Konwińska, M.; Nawrocki, M.; Huang, Y.; Bryja, A.; Celichowski, P.; Jankowski, M.; Błochowiak, K.; Mehr, K.; Bruska, M.; Nowicki, M.; et al. New Gene Markers for Metabolic Processes and Homeostasis in Porcine Buccal Pouch Mucosa during Cells Long Term-Cultivation—A Primary Culture Approach. *Int. J. Mol. Sci.* **2018**, *19*, 1027. [[CrossRef](#)] [[PubMed](#)]
27. Hayashi, Y.; Murakami, M.; Kawamura, R.; Ishizaka, R.; Fukuta, O.; Nakashima, M. CXCL14 and MCP1 are potent trophic factors associated with cell migration and angiogenesis leading to higher regenerative potential of dental pulp side population cells. *Stem Cell Res. Ther.* **2015**, *6*, 111. [[CrossRef](#)] [[PubMed](#)]
28. Sackmann-Sala, L.; Guidotti, J.E.; Goffin, V. Minireview: Prolactin regulation of adult stem cells. *Mol. Endocrinol.* **2015**, *29*, 667–681. [[CrossRef](#)] [[PubMed](#)]

29. Ruan, B.; Zhu, Z.; Yan, Z.; Yang, W.; Zhai, D.; Wang, L.; Ye, Z.; Lu, H.; Xiang, A.; Liang, J.; et al. Azoramidate, a novel regulator, favors adipogenesis against osteogenesis through inhibiting the GLP-1 receptor-PKA- β -catenin pathway. *Stem Cell Res. Ther.* **2018**, *9*. [[CrossRef](#)] [[PubMed](#)]
30. Kobayashi, S.; Fukuhara, A.; Otsuki, M.; Suganami, T.; Ogawa, Y.; Morii, E.; Shimomura, I. Fat/vessel-derived secretory protein (Favine)/CCDC3 is involved in lipid accumulation. *J. Biol. Chem.* **2015**, *290*, 7443–7451. [[CrossRef](#)]
31. Liao, W.; Liu, H.; Zhang, Y.; Jung, J.H.; Chen, J.; Su, X.; Kim, Y.C.; Flores, E.R.; Wang, S.M.; Czarny-Ratajczak, M.; et al. Ccdc3: A new P63 target involved in regulation of liver lipid metabolism. *Sci. Rep.* **2017**, *7*. [[CrossRef](#)]
32. Takeuchi, M.; Higashino, A.; Takeuchi, K.; Hori, Y.; Koshihata-Takeuchi, K.; Makino, H.; Monobe, Y.; Kishida, M.; Adachi, J.; Takeuchi, J.; et al. Transcriptional dynamics of immortalized human mesenchymal stem cells during transformation. *PLoS ONE* **2015**, *10*. [[CrossRef](#)]
33. Bae, S.; Ahn, J.H.; Park, C.W.; Son, H.K.; Kim, K.S.; Lim, N.K.; Jeon, C.J.; Kim, H. Gene and microRNA expression signatures of human mesenchymal stromal cells in comparison to fibroblasts. *Cell Tissue Res.* **2009**, *335*, 565–573. [[CrossRef](#)]
34. Secco, M.; Moreira, Y.B.; Zucconi, E.; Vieira, N.M.; Jazedje, T.; Muotri, A.R.; Okamoto, O.K.; Verjovski-Almeida, S.; Zatz, M. Gene expression profile of mesenchymal stem cells from paired umbilical cord units: Cord is different from blood. *Stem Cell Rev. Reports* **2009**, *5*, 387–401. [[CrossRef](#)]
35. Gómez, C.; Jimeno, D.; Fernández-Medarde, A.; García-Navas, R.; Calzada, N.; Santos, E. Ras-GRF2 regulates nestin-positive stem cell density and onset of differentiation during adult neurogenesis in the mouse dentate gyrus. *Mol. Cell. Neurosci.* **2017**, *85*, 127–147. [[CrossRef](#)]
36. Fideles, S.O.M.; Ortiz, A.C.; Assis, A.F.; Duarte, M.J.; Oliveira, F.S.; Passos, G.A.; Beloti, M.M.; Rosa, A.L. Effect of cell source and osteoblast differentiation on gene expression profiles of mesenchymal stem cells derived from bone marrow or adipose tissue. *J. Cell. Biochem.* **2019**, *120*, 11842–11852. [[CrossRef](#)]
37. Lin, H.; Du, Q.; Li, Q.; Wang, O.; Wang, Z.; Liu, K.; Akert, L.; Zhang, C.; Chung, S.; Duan, B.; et al. Differentiating human pluripotent stem cells into vascular smooth muscle cells in three dimensional thermoreversible hydrogels. *Biomater. Sci.* **2019**, *7*, 347–361. [[CrossRef](#)]
38. Caley, M.P.; Martins, V.L.C.; O’Toole, E.A. Metalloproteinases and Wound Healing. *Adv. Wound Care* **2015**, *4*, 225–234. [[CrossRef](#)]
39. Von der Heyde, B.; Emmanouilidou, A.; Mazzaferro, E.; Vicenzi, S.; Höijer, I.; Klingström, T.; Jumaa, S.; Dethlefsen, O.; Snieder, H.; de Geus, E.; et al. Translating GWAS-identified loci for cardiac rhythm and rate using an in vivo image- and CRISPR/Cas9-based approach. *Sci. Rep.* **2020**, *10*, 1–18. [[CrossRef](#)]
40. Ackema, K.B.; Charité, J. Mesenchymal stem cells from different organs are characterized by distinct topographic Hox codes. *Stem Cells Dev.* **2008**, *17*, 979–991. [[CrossRef](#)]
41. Bhatlekar, S.; Fields, J.Z.; Boman, B.M. Role of HOX genes in stem cell differentiation and cancer. *Stem Cells Int.* **2018**, *2018*. [[CrossRef](#)]
42. Deng, P.; Yu, Y.; Hong, C.; Wang, C.Y. Growth differentiation factor 6, a repressive target of EZH2, promotes the commitment of human embryonic stem cells to mesenchymal stem cells. *Bone Res.* **2020**, *8*. [[CrossRef](#)]
43. Wang, S.S.; Huang, H.Y.; Chen, S.Z.; Li, X.; Zhang, W.T.; Tang, Q.Q. Gdf6 induces commitment of pluripotent mesenchymal C3H10T1/2 cells to the adipocyte lineage. *FEBS J.* **2013**, *280*, 2644–2651. [[CrossRef](#)] [[PubMed](#)]
44. Calloni, R.; Cordero, E.A.A.; Henriques, J.A.P.; Bonatto, D. Reviewing and updating the major molecular markers for stem cells. *Stem Cells Dev.* **2013**, *22*, 1455–1476. [[CrossRef](#)]
45. Hofsteen, P.; Robitaille, A.M.; Strash, N.; Palpant, N.; Moon, R.T.; Pabon, L.; Murry, C.E. ALPK2 Promotes Cardiogenesis in Zebrafish and Human Pluripotent Stem Cells. *iScience* **2018**, *2*, 88–100. [[CrossRef](#)]
46. Bogomolovas, J.; Feng, W.; Yu, M.D.; Huang, S.; Zhang, L.; Trexler, C.; Gu, Y.; Spinuzzi, S.; Chen, J. Atypical ALPK2 kinase is not essential for cardiac development and function. *Am. J. Physiol. - Heart Circ. Physiol.* **2020**, *318*, H1509–H1515. [[CrossRef](#)]
47. Chan, S.F.; Huang, X.; McKercher, S.R.; Zaidi, R.; Okamoto, S.I.; Nakanishi, N.; Lipton, S.A. Transcriptional profiling of MEF2-regulated genes in human neural progenitor cells derived from embryonic stem cells. *Genomics Data* **2015**, *3*, 24–27. [[CrossRef](#)] [[PubMed](#)]
48. Nargesi, A.A.; Lerman, L.O.; Eirin, A. Mesenchymal Stem Cell-derived Extracellular Vesicles for Renal Repair. *Curr. Gene Ther.* **2017**, *17*. [[CrossRef](#)]
49. Lai, R.C.; Tan, S.S.; Teh, B.J.; Sze, S.K.; Arslan, F.; de Kleijn, D.P.; Choo, A.; Lim, S.K. Proteolytic Potential of the MSC Exosome Proteome: Implications for an Exosome-Mediated Delivery of Therapeutic Proteasome. *Int. J. Proteomics* **2012**, *2012*, 1–14. [[CrossRef](#)]
50. Oñate, B.; Vilahur, G.; Camino-López, S.; Díez-Caballero, A.; Ballesta-López, C.; Ybarra, J.; Moscattiello, F.; Herrero, J.; Badimon, L. Stem cells isolated from adipose tissue of obese patients show changes in their transcriptomic profile that indicate loss in stemcellness and increased commitment to an adipocyte-like phenotype. *BMC Genomics* **2013**, *14*. [[CrossRef](#)]
51. Finnegan, A.; Cho, R.J.; Luu, A.; Harirchian, P.; Lee, J.; Cheng, J.B.; Song, J.S. Single-cell transcriptomics reveals spatial and temporal turnover of keratinocyte differentiation regulators. *Front. Genet.* **2019**, *10*. [[CrossRef](#)] [[PubMed](#)]
52. Onizuka, S.; Iwata, T.; Park, S.; Nakai, K.; Yamato, M.; Okano, T.; Izumi, Y. ZBTB16 as a Downstream Target Gene of Osterix Regulates Osteoblastogenesis of Human Multipotent Mesenchymal Stromal Cells. *J. Cell. Biochem.* **2016**, *117*, 2423–2434. [[CrossRef](#)]

53. Marofi, F.; Vahedi, G.; Solali, S.; Alivand, M.; Salarinasab, S.; Zadi Heydarabad, M.; Farshdousti Hagh, M. Gene expression of TWIST1 and ZBTB16 is regulated by methylation modifications during the osteoblastic differentiation of mesenchymal stem cells. *J. Cell. Physiol.* **2019**, *234*, 6230–6243. [\[CrossRef\]](#)
54. Li, X.; Liu, P.; Liu, W.; Maye, P.; Zhang, J.; Zhang, Y.; Hurley, M.; Guo, C.; Boskey, A.; Sun, L.; et al. Dkk2 has a role in terminal osteoblast differentiation and mineralized matrix formation. *Nat. Genet.* **2005**, *37*, 945–952. [\[CrossRef\]](#)
55. Hwang, J.Y.; Lee, S.H.; Kim, G.S.; Koh, J.M.; Go, M.J.; Kim, Y.J.; Kim, H.C.; Kim, T.H.; Hong, J.M.; Park, E.K.; et al. HSD11B1 polymorphisms predicted bone mineral density and fracture risk in postmenopausal women without a clinically apparent hypercortisolemia. *Bone* **2009**, *45*, 1098–1103. [\[CrossRef\]](#)
56. Eijken, M.; Hewison, M.; Cooper, M.S.; de Jong, F.H.; Chiba, H.; Stewart, P.M.; Uitterlinden, A.G.; Pols, H.A.P.; van Leeuwen, J.P.T.M. 11 β -Hydroxysteroid Dehydrogenase Expression and Glucocorticoid Synthesis Are Directed by a Molecular Switch during Osteoblast Differentiation. *Mol. Endocrinol.* **2005**, *19*, 621–631. [\[CrossRef\]](#)
57. Lee, H.; Lee, Y.J.; Choi, H.; Seok, J.W.; Yoon, B.K.; Kim, D.; Han, J.Y.; Lee, Y.; Kim, H.J.; Kim, J.W. SCARA5 plays a critical role in the commitment of mesenchymal stem cells to adipogenesis. *Sci. Rep.* **2017**, *7*. [\[CrossRef\]](#)
58. Palmieri, A.; Pezzetti, F.; Graziano, A.; Riccardo, D.; Zollino, I.; Brunelli, G.; Martinelli, M.; Arlotti, M.; Carinci, F. Comparison between osteoblasts derived from human dental pulp stem cells and osteosarcoma cell lines. *Cell Biol. Int.* **2008**, *32*, 733–738. [\[CrossRef\]](#)
59. Chen, K.; Xie, S.; Jin, W. Crucial lncRNAs associated with adipocyte differentiation from human adiposederived stem cells based on co-expression and ceRNA network analyses. *PeerJ* **2019**, *2019*, e7544. [\[CrossRef\]](#)
60. Markway, B.D.; Cho, H.; Zilberman-Rudenko, J.; Holden, P.; McAlinden, A.; Johnstone, B. Hypoxia-inducible factor 3-alpha expression is associated with the stable chondrocyte phenotype. *J. Orthop. Res.* **2015**, *33*, 1561–1570. [\[CrossRef\]](#)
61. Bonet, F.; Pereira, P.N.G.; Bover, O.; Marques, S.; Inácio, J.M.; Belo, J.A. CCBE1 is required for coronary vessel development and proper coronary artery stem formation in the mouse heart. *Dev. Dyn.* **2018**, *247*, 1135–1145. [\[CrossRef\]](#) [\[PubMed\]](#)
62. Tadijan, A.; Samaržija, I.; Humphries, J.D.; Humphries, M.J.; Ambrović-Ristov, A. KANK family proteins in cancer. *Int. J. Biochem. Cell Biol.* **2021**, *131*.
63. Kim, I.; Kang, J.; Gee, H.Y.; Park, J.W. A novel HIF1AN substrate KANK3 plays a tumor-suppressive role in hepatocellular carcinoma. *Cell Biol. Int.* **2018**, *42*, 303–312. [\[CrossRef\]](#) [\[PubMed\]](#)
64. Hytönen, M.K.; Lohi, H. Canine models of human rare disorders. *Rare Dis.* **2016**, *4*, e1241362. [\[CrossRef\]](#)
65. Marusina, A.I.; Merleev, A.A.; Luna, J.I.; Olney, L.; Haigh, N.E.; Yoon, D.; Guo, C.; Ovadia, E.M.; Shimoda, M.; Luxardi, G.; et al. Tunable hydrogels for mesenchymal stem cell delivery: Integrin-induced transcriptome alterations and hydrogel optimization for human wound healing. *Stem Cells* **2020**, *38*, 231–245. [\[CrossRef\]](#)
66. Lin, X.; Dong, R.; Diao, S.; Yu, G.; Wang, L.; Li, J.; Fan, Z. SFRP2 enhanced the adipogenic and neuronal differentiation potentials of stem cells from apical papilla. *Cell Biol. Int.* **2017**, *41*, 534–543. [\[CrossRef\]](#)
67. Jin, L.; Cao, Y.; Yu, G.; Wang, J.; Lin, X.; Ge, L.; Du, J.; Wang, L.; Diao, S.; Lian, X.; et al. SFRP2 enhances the osteogenic differentiation of apical papilla stem cells by antagonizing the canonical WNT pathway. *Cell. Mol. Biol. Lett.* **2017**, *22*. [\[CrossRef\]](#)
68. Yang, Y.; Chen, X.H.; Li, F.G.; Chen, Y.X.; Gu, L.Q.; Zhu, J.K.; Li, P. In vitro induction of human adipose-derived stem cells into lymphatic endothelial-like cells. *Cell. Reprogram.* **2015**, *17*, 69–76. [\[CrossRef\]](#)
69. Sheikh, A.; Takatori, A.; Hossain, M.S.; Hasan, M.K.; Tagawa, M.; Nagase, H.; Nakagawara, A. Unfavorable neuroblastoma prognostic factor NLR2 inhibits cell differentiation by transcriptional induction through JNK pathway. *Cancer Sci.* **2016**, *107*, 1223–1232. [\[CrossRef\]](#)
70. Sanchez-Pulido, L.; Ponting, C.P. TMEM132: An ancient architecture of cohesin and immunoglobulin domains define a new family of neural adhesion molecules. *Bioinformatics* **2018**, *34*, 721–724. [\[CrossRef\]](#)
71. Hng, C.H.; Camp, E.; Anderson, P.; Breen, J.; Zannettino, A.; Gronthos, S. HOPX regulates bone marrow-derived mesenchymal stromal cell fate determination via suppression of adipogenic gene pathways. *Sci. Rep.* **2020**, *10*, 11345. [\[CrossRef\]](#)
72. Vidal, C.; Li, W.; Santner-Nanan, B.; Lim, C.K.; Guillemin, G.J.; Ball, H.J.; Hunt, N.H.; Nanan, R.; Duque, G. The kynurenine pathway of tryptophan degradation is activated during osteoblastogenesis. *Stem Cells* **2015**, *33*, 111–121. [\[CrossRef\]](#)
73. Griffin, J.N.; del Viso, F.; Duncan, A.R.; Robson, A.; Hwang, W.; Kulkarni, S.; Liu, K.J.; Khokha, M.K. RAPGEF5 Regulates Nuclear Translocation of β -Catenin. *Dev. Cell* **2018**, *44*, 248–260.e4. [\[CrossRef\]](#)
74. Yamada, T.; Park, C.S.; Burns, A.; Nakada, D.; Lacorazza, H.D. The cytosolic protein G0S2 maintains quiescence in hematopoietic stem cells. *PLoS ONE* **2012**, *7*. [\[CrossRef\]](#)
75. Mauffrey, P.; Tchitchek, N.; Barroca, V.; Bemelmans, A.; Firlej, V.; Allory, Y.; Roméo, P.H.; Magnon, C. Progenitors from the central nervous system drive neurogenesis in cancer. *Nature* **2019**, *569*, 672–678. [\[CrossRef\]](#)
76. Zhao, N.; Peacock, S.O.; Lo, C.H.; Heidman, L.M.; Rice, M.A.; Fahrenholtz, C.D.; Greene, A.M.; Magani, F.; Copello, V.A.; Martinez, M.J.; et al. Arginine vasopressin receptor 1a is a therapeutic target for castration-resistant prostate cancer. *Sci. Transl. Med.* **2019**, *11*. [\[CrossRef\]](#)
77. Chen, G.-L.; Ye, T.; Chen, H.-L.; Zhao, Z.-Y.; Tang, W.-Q.; Wang, L.-S.; Xia, J.-L. Xanthine dehydrogenase downregulation promotes TGF β signaling and cancer stem cell-related gene expression in hepatocellular carcinoma. *Oncogenesis* **2017**, *6*, e382. [\[CrossRef\]](#)
78. Zhang, D.L.; Sun, Y.J.; Ma, M.L.; Wang, Y.J.; Lin, H.; Li, R.R.; Liang, Z.L.; Gao, Y.; Yang, Z.; He, D.F.; et al. Gq activity-and β -arrestin-1 scaffolding-mediated ADGRG2/CFTR coupling are required for male fertility. *Elife* **2018**, *7*. [\[CrossRef\]](#)

79. Wood, C.; Rogers, P. A Pregnancy After Planned Partial Endometrial Resection. *Aust. New Zeal. J. Obstet. Gynaecol.* **1993**, *33*, 316–318. [[CrossRef](#)]
80. Cai, Z.; Liu, W.; Chen, K.; Wang, P.; Xie, Z.; Li, J.; Li, M.; Cen, S.; Ye, G.; Li, Z.; et al. Aberrantly Expressed lncRNAs and mRNAs of Osteogenically Differentiated Mesenchymal Stem Cells in Ossification of the Posterior Longitudinal Ligament. *Front. Genet.* **2020**, *11*. [[CrossRef](#)]
81. Liu, T.; Gao, Y.; Sakamoto, K.; Minamizato, T.; Furukawa, K.; Tsukazaki, T.; Shibata, Y.; Bessho, K.; Komori, T.; Yamaguchi, A. BMP-2 promotes differentiation of osteoblasts and chondroblasts in Runx2-deficient cell lines. *J. Cell. Physiol.* **2007**, *211*, 728–735. [[CrossRef](#)] [[PubMed](#)]
82. Pilgaard, L.; Lund, P.; Duroux, M.; Lockstone, H.; Taylor, J.; Emmersen, J.; Fink, T.; Ragoussis, J.; Zachar, V. Transcriptional signature of human adipose tissue-derived stem cells (hASCs) preconditioned for chondrogenesis in hypoxic conditions. *Exp. Cell Res.* **2009**, *315*, 1937–1952. [[CrossRef](#)] [[PubMed](#)]
83. Ishida, H.; Saba, R.; Kokkinopoulos, I.; Hashimoto, M.; Yamaguchi, O.; Nowotschin, S.; Shiraiishi, M.; Ruchaya, P.; Miller, D.; Harmer, S.; et al. GFRA2 Identifies Cardiac Progenitors and Mediates Cardiomyocyte Differentiation in a RET-Independent Signaling Pathway. *Cell Rep.* **2016**, *16*, 1026–1038. [[CrossRef](#)] [[PubMed](#)]
84. Qian, X.; Wagner, S.; Ma, C.; Coordes, A.; Gekeler, J.; Klussmann, J.P.; Hummel, M.; Kaufmann, A.M.; Albers, A.E. Prognostic significance of ALDH1A1-positive cancer stem cells in patients with locally advanced, metastasized head and neck squamous cell carcinoma. *J. Cancer Res. Clin. Oncol.* **2014**, *140*, 1151–1158. [[CrossRef](#)]
85. Palmieri, F. The mitochondrial transporter family SLC25: Identification, properties and physiopathology. *Mol. Aspects Med.* **2013**, *34*, 465–484. [[CrossRef](#)]
86. Jiang, H.; Lei, R.; Ding, S.W.; Zhu, S. Skewer: A fast and accurate adapter trimmer for next-generation sequencing paired-end reads. *BMC Bioinformatics* **2014**, *15*, 182. [[CrossRef](#)]
87. Yates, A.D.; Achuthan, P.; Akanni, W.; Allen, J.; Allen, J.; Alvarez-Jarreta, J.; Amode, M.R.; Armean, I.M.; Azov, A.G.; Bennett, R.; et al. Ensembl 2020. *Nucleic Acids Res.* **2020**, *48*, D682–D688. [[CrossRef](#)]
88. Kõressaar, T.; Lepamets, M.; Kaplinski, L.; Raime, K.; Andreson, R.; Remm, M. Primer3-masker: Integrating masking of template sequence with primer design software. *Bioinformatics* **2018**, *34*, 1937–1938. [[CrossRef](#)]
89. Rao, X.; Huang, X.; Zhou, Z.; Lin, X. An improvement of the $2^{(-\Delta\Delta CT)}$ method for quantitative real-time polymerase chain reaction data analysis. *Biostat. Bioinforma. Biomath.* **2013**, *3*, 71–85.
90. Ge, S.X.; Son, E.W.; Yao, R. iDEP: An integrated web application for differential expression and pathway analysis of RNA-Seq data. *BMC Bioinformatics* **2018**, *19*, 1–24. [[CrossRef](#)]
91. Robinson, M.D.; McCarthy, D.J.; Smyth, G.K. edgeR: A Bioconductor package for differential expression analysis of digital gene expression data. *Bioinformatics* **2010**, *26*, 139–140. [[CrossRef](#)]
92. Von Mering, C.; Jensen, L.J.; Snel, B.; Hooper, S.D.; Krupp, M.; Foglierini, M.; Jouffre, N.; Huynen, M.A.; Bork, P. STRING: Known and predicted protein-protein associations, integrated and transferred across organisms. *Nucleic Acids Res.* **2004**, *33*, D433–D437. [[CrossRef](#)]